Theoretical and experimental comparison of SnPc, PbPc, and CoPc adsorption on Ag(111)

J. D. Baran and J. A. Larsson
Tyndall National Institute, University College Cork, Lee Maltings, Prospect Row, Cork, Ireland

R. A. J. Woolley, Yan Cong, and P. J. Moriarty
The School of Physics and Astronomy, The University of Nottingham, Nottingham NG7 2RD, United Kingdom

A. A. Cafolla
School of Physical Sciences, Dublin City University, Glasnevin, Dublin 9, Ireland

K. Schulte
MAX-lab, Lund University, P.O. Box 118, SE-221 00 Lund, Sweden

V. R. Dhanak
Department of Physics, University of Liverpool, Liverpool L69 3BX, United Kingdom
(Received 17 July 2009; revised manuscript received 4 January 2010; published 16 February 2010)

A combination of normal-incidence x-ray standing-wave (NIXSW) spectroscopy, x-ray photoelectron spectroscopy (XPS), scanning tunneling microscopy (STM), and density-functional theory (DFT) has been used to investigate the interaction of a number of phthalocyanine molecules (specifically, SnPc, PbPc, and CoPc) with the Ag(111) surface. The metal-surface distances predicted by the DFT calculations for SnPc/Ag(111) (2.48 Å) and CoPc/Ag(111) (2.88 Å) are in good agreement with our NIXSW experimental results for these systems (2.31 ± 0.09 and 2.90 ± 0.05 Å, respectively). Good agreement is also found between calculated partial density-of-states plots and STM images of CoPc on Ag(111). Although the DFT and Pb $4f$ NIXSW results for the Pb-Ag(111) distance are similarly in apparently good agreement, the Pb $4f$ core-level data suggest that a chemical reaction between PbPc and Ag(111) occurs due to the annealing procedure used in our experiments and that the similarity of the DFT and Pb $4f$ NIXSW values for the Pb-Ag(111) distance is likely to be fortuitous. We interpret the Pb $4f$ XPS data as indicating that the Pb atom can detach from the PbPc molecule when it is adsorbed in the "Pb-down" position, leading to the formation of a Pb-Ag alloy and the concomitant reduction in Pb from a Pb^{2+} state (in bulklike films of PbPc) to Pb^0. In contrast to SnPc, neither PbPc nor CoPc forms a well-ordered monolayer on Ag(111) via the deposition and annealing procedures we have used. Our DFT calculations show that each of the phthalocyanine molecules donate charge to the silver surface, and that back donation from Ag to the metal atom (Co, Sn, or Pb) is only significant for CoPc.

DOI: 10.1103/PhysRevB.81.075413 PACS number(s): 68.05.Cf, 68.08.Bc, 61.46.Df

I. INTRODUCTION

Metal phthalocyanine (MPc) molecules play a central role in the study of organic-inorganic interfaces and, more broadly, in the field of molecular electronics. This is largely due to their high thermal stability and ease of sublimation,[1] their propensity to form well-ordered assemblies on a variety of solid surfaces,[2–7] and their fascinating and tunable (opto-)electronic properties.[8] MPcs have also been the subject of a variety of pioneering single molecule imaging, spectroscopy, and manipulation experiments, ranging from the seminal work of Gimzewski *et al.*[9] and Lippel *et al.*[10] on imaging intramolecular features using the scanning tunneling microscope (STM) to the elegant experiments of Zhao *et al.*[11] and, more recently, Wang *et al.*[12] where an STM has been used to very precisely modify and engineer the internal structure of individual molecules.

As was shown particularly well by Zhao *et al.*,[11] the precise chemical and structural environment of the metal atom at the center of a MPc molecule is key to controlling the electronic properties of the molecule (and, indeed, the local environment of the molecule). STM measures the local density of states (within an energy window whose width is determined by the bias voltage applied to the sample or tip) and it is thus problematic at best to extract a "true" molecule-substrate or M-substrate separation from STM data alone. A number of researchers have therefore used the x-ray standing-wave (XSW) spectroscopy technique to determine the separation of both the central metal atom and the molecular "framework" from the underlying surface on which its adsorbed: Gerlach *et al.*[13] carried out a detailed study of adsorption-induced distortion of perfluorinated copper phthalocyanine molecules and Stadler *et al.*[5] had determined the structure of SnPc adsorbed on Ag(111) using photoemission-based XSW [their measured value for the Sn-Ag(111) separation of 2.41 Å was reproduced in an Auger-based XSW study of the SnPc/Ag(111) by our group[6]]. Stadler *et al.*[14] had also recently used normal-incidence x-ray standing-wave spectroscopy (NIXSW) to examine how intermolecular interactions can be tuned in SnPc (sub)monolayers on Ag(111).

Here we present the results of a combined experimental and theoretical study of the adsorption of three different MPc molecules, CoPc, PbPc, and SnPc, on the Ag(111) surface. The predictions of density-functional theory (DFT) calculations are compared with the results of NIXSW spectroscopy, STM, and x-ray photoelectron spectroscopy mea-

surements of a 1 monolayer (ML) coverage of each phthalocyanine molecule on the silver surface. Unlike SnPc, neither CoPc nor PbPc forms a well-ordered monolayer under the deposition and annealing conditions used in our study. (This proviso is important given the kinetic limitations observed in the assembly of phthalocyanine monolayers in previous studies). For CoPc, however, there is a relatively high level of order associated with the positions of the Co atoms with respect to their vertical separation from the underlying Ag(111) surface, indicating that the majority of molecules adsorb in a similar configuration with regard to the placement of the Co atom. A similarly high level of coherence has been observed in previous XSW studies of the SnPc/Ag(111) system. For PbPc, the coherence is markedly lower and, when the NIXSW results are considered in parallel with XPS and STM data, suggests that the Pb atoms for those molecules adsorbed in the "Pb down" configuration react with the underlying Ag(111) surface, forming a Pb-Ag alloy.

We highlight at this point the recent work of Stadler *et al.*[14] which has shown that there can be a significant coverage dependence for SnPc interactions on the Ag(111) surface. Given that the primary goal of our experimental measurements and theoretical calculations was an intercomparison of the adsorption properties of different MPc molecules we have striven to treat all three molecules on an "equal footing" in terms of sample preparation and the setup of the molecule-substrate clusters used in the DFT work. As such, we have aimed to prepare a 1 ML coverage [via deposition onto the Ag(111) surface held at 300 °C] and have considered only isolated MPc molecules in the DFT calculations. Given the results of Stadler *et al.* for the SnPc-Ag(111) system, however, it is likely that the use of different molecular coverages could modify the XSW results.

II. DENSITY-FUNCTIONAL THEORY

There has been some discussion of how best to describe the *d* levels of the central transition-metal atom of porphyrin and phthalocyanine molecules,[15–18] but no consensus has yet been reached. Using the TURBOMOLE (Ref. 19) package we have performed first-principles calculations using unrestricted DFT with the generalized gradient approximation (GGA) parametrization by Perdew-Burke-Ernzerhof (PBE) for the exchange-correlation energy[20] and the resolution-of-the-identity (RI) approximation.[21,22] The basis sets are double-zeta split valence augmented by polarization function DZVP2, for all atoms except Sn and Pb for which larger triple-zeta split valences, augmented by the double polarization function TZVPP2, are used to describe the complex nature of the electronic shells of these atoms. Effective core potentials (ECPs) are used to take into account scalar relativistic effects, ECP-28-MWB (Ref. 23) for Ag, ECP-28-MDF for Sn, and ECP-60-MDF (Ref. 24) for Pb.

In all calculations, we have employed a cluster representation of the Ag(111) surface to describe MPc—surface adsorption. Each system under study contains 226 atoms: one MPc molecule with 57 atoms and an Ag_{169} cluster with three layers. We used two Ag(111) cluster models. One model has an on-top site in the center on one side and a fcc-hollow site in the center of the flip side. The other model has a hcp-hollow site in the center on both sides. In addition, the free MPc molecules were optimized within the same framework. All atoms were allowed to fully relax in the geometry optimizations, which were performed with convergence criterions 10^{-6} hartree on energy and 10^{-3} bohr on gradient. In our calculations, three initial configurations with MPc adsorbed on three high-symmetry sites hcp, fcc, on-top on Ag(111) surface have been considered. We placed the center of mass of each MPc, namely, the central metal atom, on each of these sites and performed a geometry optimization.

III. EXPERIMENT

A. Overview of NIXSW

We refer the reader to review papers by Woodruff[25,26] and Zegenhagen[27] for in-depth discussions of the theory underlying NIXSW. In the following we briefly cover only the key principles of XSW. When crystal planes of spacing d_H are illuminated with x rays of wavelength λ at an angle θ, diffraction will occur, as described by the Bragg equation, $2d_H \sin\theta = n\lambda$. When this equation is satisfied, the incident and reflected wave fields interfere, producing an x-ray standing wave which penetrates into the crystal and extends well beyond the surface. To circumvent problems related to the degree of crystal perfection—in particular, the sample mosaicity—required to carry out XSW measurements, the Bragg condition's turning point at $\theta = 90°$ is exploited in normal-incidence XSW (see Ref. 25 for a discussion).

The first requirement in a standing-wave experiment is therefore to obtain a suitable standing-wave generator, usually a crystal. Suppose now that there are atoms or molecules adsorbed at the surface of the crystal. Each adsorbate will be "bathed" in the x-ray standing-wave field and will therefore emit photoelectrons, Auger electrons, and/or x-ray photons with a yield, *Y*, proportional to the x-ray intensity at the adsorbate position. The intensity of the standing-wave field at the adsorbate position can be changed by varying the photon energy (within the reflectivity region). As discussed at length by Woodruff,[25] the yield can be written as

$$Y = 1 + R + 2\sqrt{R} f_{co} \cos(\phi - 2\pi D), \tag{1}$$

where R is the x-ray reflectivity, f_{co} is the coherent fraction—a number between 0 and 1 which represents the degree of order associated with the occupation of a particular site, and D is the coherent position—the position of the adsorbate with respect to the (extended) bulk lattice planes. Triangulation of an adsorbate position can be achieved by using a number of complementary allowed reflections.

If photoelectron yield is used to monitor x-ray absorption, the contribution of higher-order (multipole) contributions beyond the standard dipole approximation must be taken into consideration.[28] The consequence for NIXSW is that the photoemission-derived yield is no longer symmetric with respect to incident and reflected x-ray wave fields.[29]

To account for the asymmetry arising from the higher-order components of the electromagnetic field—in particular, the cross terms involving the electric quadrupole and mag-

netic dipole terms, $E1\cdot E2$ and $E1\cdot M1$—an asymmetry parameter, Q (Ref. 28) has been introduced. A general formalism developed by Vartanyants and Zegenhagen[30] includes multipole effects related to matrix elements that describe the scattering process, such as the photoionization energy, initial bound electron state, and the experimental geometry (however, currently only a description for the s state is available). Lee *et al.*[31] had shown that interference terms from the more rigorous treatment in Ref. 30 have little effect on the structural parameters D and f_{co}. Here we will treat the data in terms of Q alone, an approach also adopted by Stadler *et al.*[5] in their NIXSW study of SnPc adsorption on Ag(111). While our (and Stadler *et al.*'s) NIXSW measurements involve photoemission from p or d orbitals, for which a theoretical framework is currently lacking, we note that the results of previous Auger-based[6] and photoemission-based (Sn $3d$) (Ref. 5) NIXSW experiments on an MPc/Ag(111) system have agreed within experimental error.

We can write the yield, Y, in terms of Q;

$$Y = 1 + R\frac{(1+Q)}{(1-Q)} + 2\sqrt{R}\frac{(1+Q)^{1/2}}{(1-Q)^{1/2}} f_{co}\cos(\phi - 2\pi D). \quad (2)$$

It is important to note that theoretical calculations do not have to be relied upon to determine Q. The asymmetry parameter can be derived experimentally *provided a completely disordered adsorbate overlayer can be created*. In this case $f_{co}=0$ and Eq. (2) reduces to

$$Y = 1 + \frac{1+Q}{1-Q}R. \quad (3)$$

Thus, the photoemission yield is the x-ray reflectivity multiplied by the $(1+Q)/(1-Q)$ factor.

B. Substrate and Pc overlayer preparation

The substrate, a Ag(111) single crystal, was cleaned in UHV using standard argon ion sputter and thermal annealing cycles of 550 °C. No contamination of the surface was detected using x-ray photoelectron spectroscopy (XPS). (An unmonochromated Mg Ka source was used for XPS measurements, unless otherwise stated, giving a FWHM of 1.2 eV for the Ag $3d_{5/2}$ linewidth.)

Sn-, Pb-, and Co-phthalocyanine molecules were purified by vacuum sublimation cycles[1] before being introduced into the experimental chamber. The source material was then thoroughly degassed in a standard Knudsen cell up to and just beyond the deposition temperature of 410 °C (representing a deposition rate of approximately 1 ML/min). In all evaporated films no contaminants were detected and the ratio of Me:C was found to be in reasonably close agreement with that expected from consideration of the theoretical photoemission cross sections and the composition of the molecule. Pc assemblies on the Ag(111) surface were prepared by depositing the molecules onto the substrate held at 300 °C(±30°).

The STM measurements were carried out in an Omicron variable temperature STM system using electrochemically etched tungsten tips and a Ag(111) substrate prepared as discussed above.

TABLE I. Asymmetry parameter (Q) values for the various core-level photoemission signals used in this work.

PES	Q
Co $2p$	0.15 ± 0.02
Pb $4f$	0.16 ± 0.04
C_{Pb} $1s$	0.30 ± 0.02
Sn $3d$	0.21 ± 0.02
C_{Sn} $1s$	0.22 ± 0.01

C. NIXSW: Experimental details and estimation of asymmetry parameter

NIXSW experiments were performed on beamline 4.2 at the SRS, Daresbury Laboratories, Warrington, U.K. (the SRS closed in August 2008) and beamline ID 32 at the ESRF Grenoble, France. Each NIXSW UHV chamber had a high-precision manipulator, allowing sample translation in the x,y,z directions, 360° rotation in the horizontal plane and ±90° in the azimuthal plane. The manipulator also incorporated either an electron beam (e-beam) or direct current heater. Low-energy electron diffraction (LEED) optics were available on both the Daresbury and ESRF systems. SRS Beamline 4.2 was also equipped with an XPS source and UV lamp.

Photoemission, Auger, and NIXSW spectra on BL 4.2 were recorded using a hemispherical analyzer (from PSP) with an acceptance angle of between 9° and 13° for the kinetic energies and pass energy (100 eV) used for our measurements. The analyzer was positioned at 40° to the incoming light [provided by a double crystal (InSb) monochromator]. On ID32, spectra were recorded using a hemispherical analyzer (Physical Electronics) positioned at 45° to the incoming light provided by a double crystal monochromator.

NIXSW spectra were obtained by first orienting the substrate such that at the Bragg energy the reflectivity was maximized. The subsequent standing-wave spectra were obtained by incrementally increasing the photon energy through the reflectivity region. Adsorbate and substrate NIXSW spectra were recorded simultaneously with the latter giving a measure of the Bragg position and degree of instrumental broadening. The structural quality of the crystal was assessed using LEED and NIXSW measurements of the substrate's Ag MNN and Ag $3d$ spectra. A sharp (1×1) LEED pattern with a low background was obtained, while the NIXSW structural parameters of $f_{co}=0.84\pm0.09$ and $D=0.98\pm0.02$ for the $\langle111\rangle$ reflection indicated that the mosaicity of the crystal was acceptable.

In order to determine the asymmetry parameter, Q, phthalocyanine films thick enough to mask detection of substrate photoemission were grown on the Ag(111) substrate while it was held at room temperature. This was to ensure disordered growth, indicated by the absence of any LEED pattern, suitable for calculating the Q value required[32] for fitting the C $1s$, Co $2p$, and Pb $4f$ core-level XSW spectra. The Q values are given in Table I. Interestingly, the C $1s$ associated nondipolar correction value, Q differs between the SnPc and

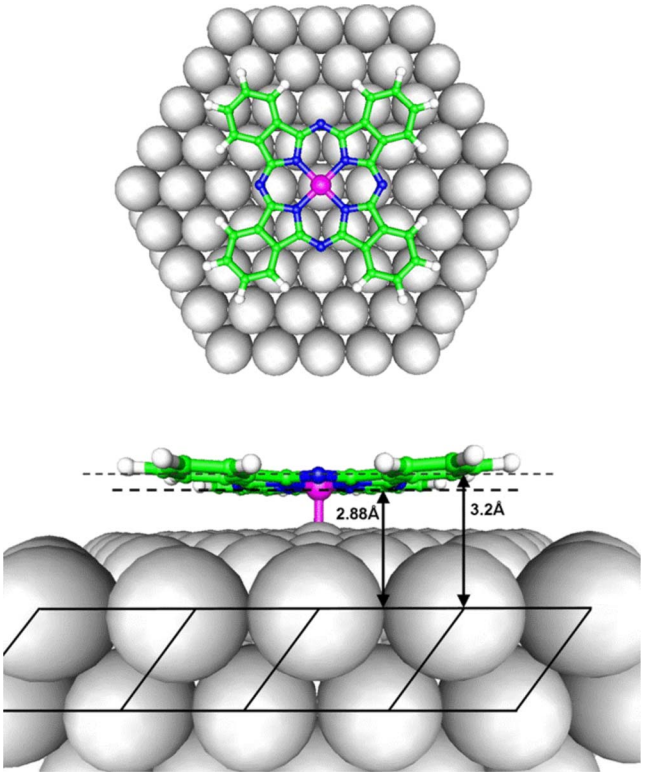

FIG. 1. (Color online) Top and side views of calculated on-top adsorption geometry of CoPc.

PbPc bulk films. Stadler *et al.*[5] also showed a lower than expected value for SnPc C 1*s* (in agreement with our own) as compared to other authors measuring phthalocyanine films on the same beamline.[13] Fisher *et al.*[28] showed in theoretical work that the C 1*s* Q parameter is 0.3. However, in some of their experimental work they also arrive at a value of 0.22. Film thickness is not thought to be the root cause for the discrepancy as SnPc and PbPc thick films are well in excess of 15 nm. Additionally, previous work with the Ce@C_{82} endofullerene[33] gave a value of 0.31 for a ML coverage. The underlying reason for the lower C 1*s* Q value in the case of SnPc is thought to stem from ordering of the molecular layers.

IV. RESULTS

A. CoPc

CoPc is a planar molecule with D_{4h} symmetry (unlike the "buckled" SnPc and PbPc molecules discussed in Secs. IV B and IV C below). Figure 1 shows top and side views of the most stable bonding geometry for CoPc on Ag(111) resulting from our DFT calculations. There is a clear preference for on-top and bridge site bonding, in stark contrast to the preference for bonding at the hcp site shown by both SnPc and PbPc. As can be discerned from Fig. 1, the CoPc molecule largely retains its planar character on adsorption with only a small distortion of the aromatic groups, manifesting as they bend away from the surface. The adsorption of CoPc leads to a significant movement of the Ag atom to which the molecule is bonded out of the surface plane (by approximately 0.3 Å). The CoPc-Ag(111) binding energy predicted by DFT is 1.40 eV and, as listed in Table II (in Sec. V), the calculated Co-Ag(111) bond length is 2.88 Å.

TABLE II. Central metal-surface and ring-surface distances in Å for MPcs adsorbed on Ag(111).

Molecule	M-surface (DFT)	Pc-surface (DFT)
CoPc	2.88	3.2
SnPc	2.48	3.7
PbPc	2.76	3.9
Molecule	M-surface (Exp.)	Pc-surface (Exp.)
CoPc	2.90(±0.05)	
SnPc	2.31(±0.09)	3.61(±0.16)
PbPc	0.47 or 2.83(±0.05)	2.93(±0.05)

NIXSW measurements of a CoPc monolayer on Ag(111) were carried out at the ESRF on beamline ID32. CoPc proved to be robust and stable despite the high flux of x-ray photons, and we did not observe any measurable degradation of the molecule [as opposed to the significant beam damage we have observed for other large organic molecules we have previously studied on ID32 (Ref. 34)]. We used Co 2*p* photoemission as the NIXSW "probe" and, as discussed in Sec. II, estimated the Q value from NIXSW profiles for thick films of CoPc. Figure 2 shows the Co 2*p* and Ag MNN NIXSW profiles for a monolayer of CoPc on Ag(111). The best fit of the Co 2*p* data to dynamical theory yields a Co-Ag(111) distance of 2.90±0.05 Å, in remarkably good agreement with the DFT result, and a coherent fraction of 0.84±0.05. (Unfortunately, for the CoPc experiment, C 1*s*

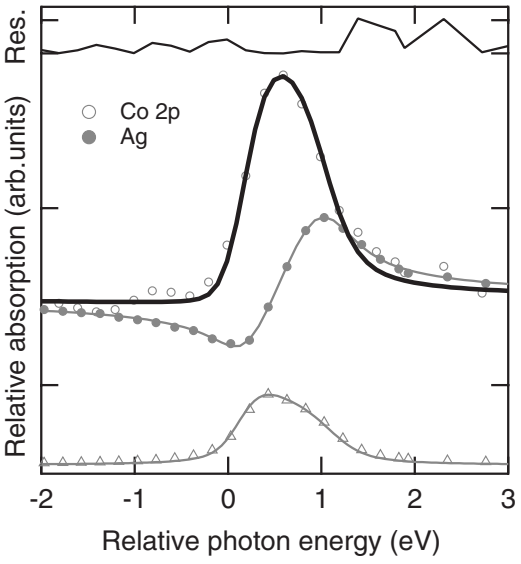

FIG. 2. (111) NIXSW profiles for a 1 ML coverage of CoPc on Ag(111). Upper plots: open circles show the Co 2*p* NIXSW data with the fit shown as a bold line; filled circles show the Ag(111) NIXSW profile for the clean surface (fit shown as a light gray line). From these data, the Co atom is 2.90±0.05 Å above the Ag(111) surface. Lower plot: reflectivity curve.

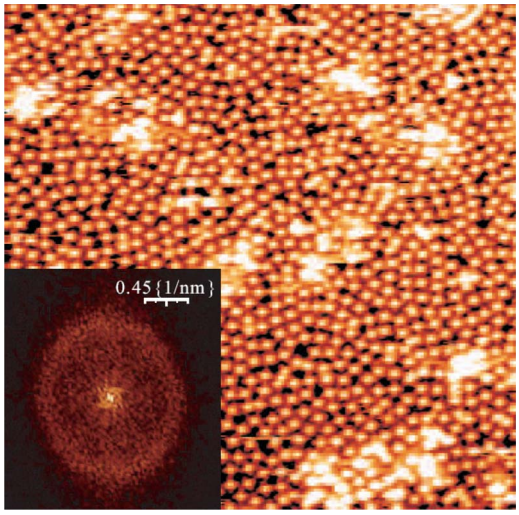

FIG. 3. (Color online) 50×50 nm^2 STM image of the CoPc monolayer (tunneling parameters: −1.1 V and 0.08 nA). Inset: Fourier transform of the image.

NIXSW data with adequate signal-to-noise ratio were not acquired.)

For all but one of the experiments we carried out (both NIXSW spectroscopy and, as detailed below, STM) we did not observe a LEED pattern for a monolayer coverage of CoPc on Ag(111). On a single occasion, however, a weak LEED pattern was observed for the first deposition of a CoPc monolayer (onto a surface held at 300 °C) using a new (but thoroughly degassed) "charge" of material in the evaporation cell. Repeated attempts to reproduce the pattern were unsuccessful. This may point to the importance of temperature-dependent kinetic limitations in forming well-ordered CoPc assemblies. Similar arguments have recently been made by Chang *et al.* for phthalocyanine adsorption on metals[35] and it is clear from work on SnPc (Refs. 5, 6, and 14) that there is a rich parameter space underpinning the self-assembly of phthalocyanines on metal surfaces.

STM images of a CoPc monolayer on Ag(111) are shown in Fig. 3. A Fourier transform of Fig. 3(a) is shown in the inset to the figure. A clear ring, betraying the presence of a well-defined correlation length, is observed but there are no clear spots observed, indicative of a lack of orientational order. While it is possible to identify regions of short-range order in Fig. 3, it is clear that the monolayer is far from well ordered. Moreover, this disorder appears to be static rather than dynamic and thus represents a "quenched" or "frozen-in" molecular gas phase rather than the lattice gas observed by Berner *et al.*[36] for two-dimensional (2D) phases of subphthalocyanine molecules on Ag(111). In addition, in our case the Fourier transform is not representative of a liquid-like structure factor. There are many similarities between the disordered phase observed in Fig. 3(a) and that observed by Lackinger and Hietschold for SnPc on Ag(111). As those authors point out, similar disordered phases have been observed for SnPc on graphite[37] and CuPc on Ag(110).[38]

The acquisition of both NIXSW and STM data for the CoPc system enables us to address a perennial question associated with the imaging of phthalocyanine molecules: to

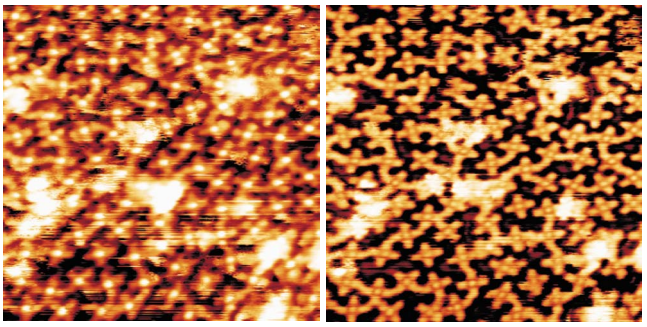

FIG. 4. (Color online) CoPc on Ag(111) imaged in; left: the forward direction with a sample bias of −1.1 and right: reverse direction biased at +0.5 V. The tunnel current was 0.15 nA in both 15×15 nm^2 images.

what extent does the apparent height of the central metal atom above the substrate surface, as measured by STM, differ from the true "topographic" height? Figure 4 shows STM images taken with positive and negative sample bias respectively where it is clear that the electronic structure of the molecule strongly influences the measured "height" of the Co atom. As pointed out by Hipps, Lu *et al.*,[39,40] STM imaging of adsorbed phthalocyanine molecules is strongly dependent on the metal *d*-orbital participation in the frontier molecular orbitals [i.e., highest occupied molecular orbital (HOMO) and lowest unoccupied molecular orbital (LUMO)] closest to the Fermi level. This is particularly important for CoPc where cobalt has a d^7 configuration and where the partially filled d_{z^2} orbital or the (d_{xz},d_{yz}) orbital pair give rise to an enhanced contrast above the center of the CoPc molecules.[40] In our case, for filled state images taken with a bias voltage of −1.1 V, the central Co atom appears $130(\pm10)$ pm above the Ag(111) surface. [We stress that this is a lower limit as the measurements were taken for a relatively high CoPc coverage where the finite radius of curvature of the tip affects the determination of the apparent height of the Co atoms above the Ag(111) surface.] This value should be compared both with the apparent height of Co above the Au(111) surface in the CoPc/Au(111) STM data reported by Lu *et al.*[40] (0.35 nm) and the value of the Co-Ag(111) separation determined from the NIXSW data shown in Fig. 2. A very crude estimate of the height of the Co atom "above" the Ag(111) surface can be made by subtracting the covalent radius of Ag (134 p.m.) from the Co-Ag(111) value determined from the XSW measurements, yielding an "apparent height" of 150 ± 10 pm. It is of course, highly likely that the agreement between the STM- and NIXSW-derived "apparent height" values in this case is entirely fortuitous. Future work, based on combined DFT simulations and STM measurements of the CoPc/Ag(111) system, will focus on elucidating the relationship between the applied bias voltage and the apparent height of the Co atom at the center of the Pc molecule.

From a comparison of filled- and empty-states images for CoPc adsorbed on Ag(111) (Fig. 4) it is clear that there is a significant filled state density (relative to that of the molecular framework) within an energy window of 1.1 eV below the Fermi level which is associated with the central Co atom. In

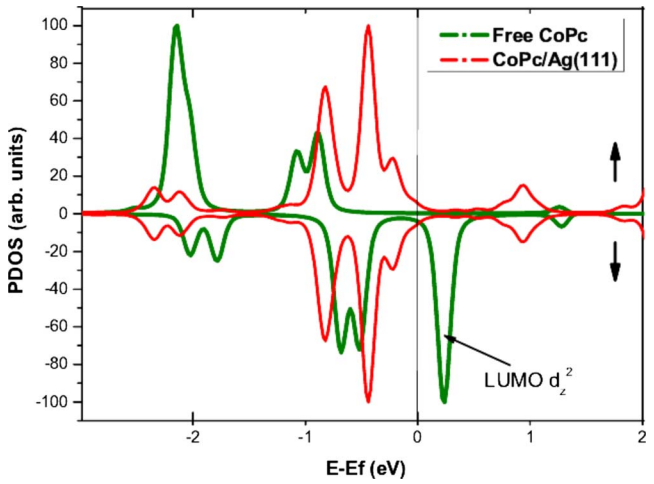

FIG. 5. (Color online) Spin-polarized PDOS of Co atom in the free CoPc molecule [green (light gray) curve] and following adsorption of CoPc on Ag(111) [red (dark gray) curve].

the filled states image acquired at 0.5 V, the Co atom appears at the same apparent height as the surrounding aromatic groups of the phthalocyanine molecule.

Our DFT calculations of the CoPc/Ag(111) system are consistent with previous studies of CoPc/Au(111),[11] which show that the interaction between the molecule and substrate clearly changes the electronic structure and magnetic moment of the adsorbed CoPc molecule. In the CoPc/Ag(111) adsorption system the magnetic moment due to one unpaired *d* electron of the Co atom is completely quenched by the molecule substrate interaction (see Fig. 5). This disappearance can be explained as a direct charge-density transfer from silver *sp* states to the previously unoccupied CoPc valence state, in particular to the LUMO of d_{z^2} character.[41–43] The preferred binding site of CoPc on Ag(111) is dictated by the Co atom, which coordinates to the silver surface by its *d* orbitals, particularly d_{z^2}. Due to the symmetry of the d_{z^2} orbital the most favorable overlap with the silver states is when Co is bonded directly to a silver atom (on-top binding site), i.e., the Co d_{z^2} interaction dominates over the interaction of nitrogen p_z orbitals with the Ag $d_{(yz)(xz)}$ states. This latter interaction produces hollow site binding on other surfaces.[18]

A comparison of the partial density of states (PDOS) for CoPc/Ag(111) for both filled and empty states within a 1 eV window above and below the Fermi level (see Fig. 6) shows that in the occupied region between 0 and 1 eV there are eight orbitals with a Co 3*d* contribution (five with $3d_{z^2}$ character, at −0.034 eV, −0.152 eV, −0.223 eV, −0.740 eV, and −0.773 eV), two orbitals with $3d_{xz(yz)}$ character (−0.439 eV and −0.442 eV), and an orbital with d_{xy} character at −0.834 eV. There is only a small contribution of the 3*d*-Co orbitals to the unoccupied density of states. We have calculated STM images at a bias voltage of −1.1 and +1.1 eV bias using the DFT wave function, i.e., neglecting interaction between the tip and the surface. Figure 6(a), which corresponds to a −1.1 eV bias, shows clearly that there is a large charge density located on the Co atom, in contrast to the +1.1 eV bias. The DFT results are therefore in good qualitative agreement with the STM data shown in Fig. 4.

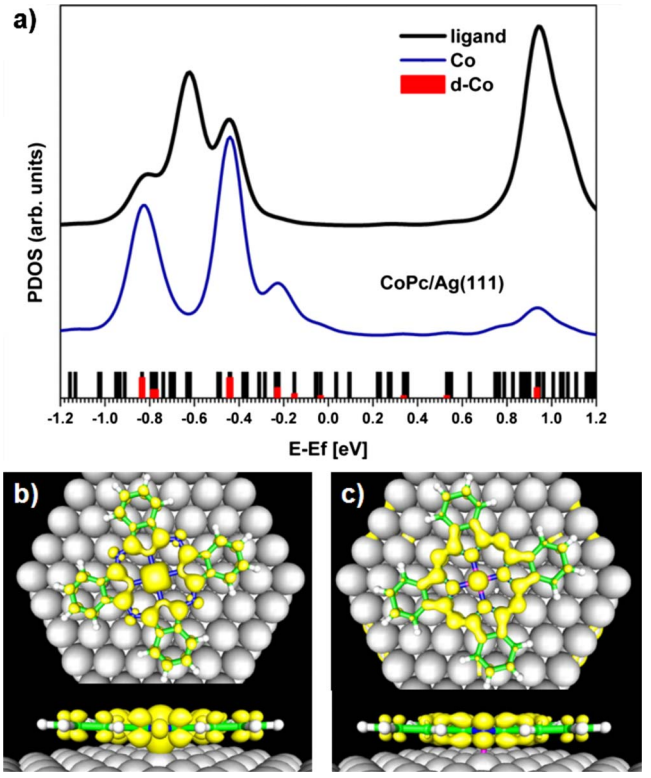

FIG. 6. (Color online) (a) PDOS of ligand and Co atom, and energy level diagram of the CoPc/Ag(111) system. The length of the red (light gray) bars represents the *d* orbital population of Co; [(b) and (c)] Top and side view of simulated STM image at (b) −1.1 eV and (c) +1.1 eV bias voltage.

B. SnPc

NIXSW and STM data for (sub)monolayer coverages of SnPc on Ag(111) have been previously published and discussed at length.[4,5,14] Here we briefly summarize previously published NIXSW and STM results before moving on to compare the results of our DFT calculations with those data.

Stadler *et al.*[5,14] had carried out careful and comprehensive investigations of the various incommensurate and commensurate phases formed by mononolayer and submonolayer coverages of SnPc on Ag(111). An incommensurate monolayer formed at room temperature, with the Pc molecules adsorbed in a "Sn down" geometry with a Sn-Ag(111) separation of ~2.41 Å. The Sn atom was found to be located ≈0.8 Å below the carbon and nitrogen atoms and there was a significant "backbending" of the benzene rings of the molecule toward the surface. For a submonolayer (0.68–0.88 ML) film cooled to 150 K, Stadler *et al.*[5] found that SnPc assembled in a commensurate phase involving a mixture of "Sn up" or "Sn down" molecules. In this phase, assuming that both adsorption geometries were equally probable (and had an associated coherent fraction of 0.9), Stadler *et al.*[5] determined the Sn-Ag(111) separation (averaged from the results for two different samples) as 2.48 Å for the "Sn-down" molecules and 3.96 Å for the "Sn-up" configuration.

Stadler *et al.* used photoemission-based NIXSW to determine the Sn-Ag(111) separation. In an Auger-based NIXSW study,[6] we reproduced (within experimental error) the Sn-

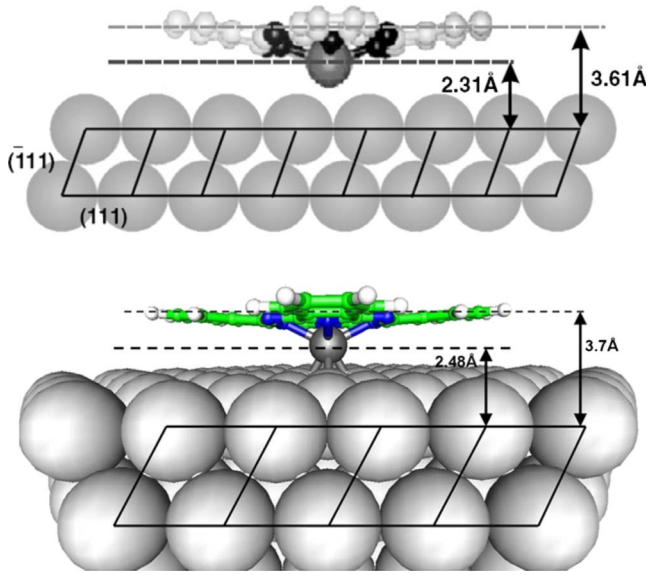

FIG. 7. (Color online) A comparison of the SnPc-Ag(111) distances determined from (upper) experiment and (lower) DFT.

Ag(111) separation of 2.41 Å reported by Stadler *et al.*[5] for SnPc on Ag(111). We used, however, a slightly different method of sample preparation—deposition onto a substrate held at 300 °C rather than postdeposition annealing—which led to some subtle differences in the self-assembly of the Pc molecules. In particular, we observed a rather counterintuitive bending of the benzene rings of the molecule *away* rather than toward the Ag(111) surface (as was reported by Stadler *et al.*[5]). Figure 7(a) shows the adsorption geometry for SnPc on Ag(111) (for an adsorbed layer prepared by molecular deposition onto a substrate held at 300 °C) determined from our NIXSW measurements.

The results of our DFT calculations indicate that adsorption of SnPc on Ag(111) induces significant distortions in the puckering of the Pc part of the molecule, as compared to the free molecule (see Fig. 8). The Sn-Ag(111) distance predicted by DFT is 2.48 Å, a value which is close to, but slightly larger than our experimentally measured value of 2.31 ± 0.09 Å and that of Stadler *et al.* We note at this point that our DFT calculations do not properly account for the dispersion interactions (instantaneous induced dipoles) between the Pc molecule and the Ag(111) surface. However, dispersion is the smallest of the attractive intermolecular forces and DFT performs reasonably well for electrostatic and polarization interactions which are more prominent in the case of a molecule with a pronounced dipole (multipole) moment with a metal surface (where the covalent contribution to the binding energy is largest). We expect a slight increase in the binding energy and a slight decrease in the adsorption distances MPc-Ag(111) for the case where dispersion is properly included.

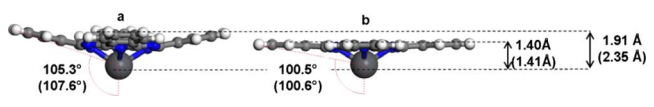

FIG. 8. (Color online) Differences in SnPc and PbPc geometry after adsorption, PbPc values in parenthesis: (a) free SnPc (PbPc) and (b) SnPc (PbPc) on Ag_{169} for hcp-hollow adsorption model.

For an isolated molecule on the Ag(111) surface, at least, the DFT results show that SnPc becomes flatter and the molecular plane is almost parallel to the surface. This can be seen in the measure of the height of the free and adsorbed metal phthalocyanine and the "shuttle-cock angle" (i.e., the angle between the outermost hydrogens and the central metal atom with regard to the Ag surface normal) (Fig. 7). The distance from the central metal atom to the outermost hydrogens, a measure of the height of the molecule, and the angle between these hydrogens and the central metal atom with regard to the Ag surface normal for adsorbed SnPc and PbPc are 1.4 Å and 100.5° and 1.41 Å and 100.6°, respectively, as compared to 1.91 Å and 105.3°, and 2.35 Å and 107.6° for the free SnPc and PbPc molecule, respectively.

C. PbPc

PbPc has a similar "shuttlecock" shape to SnPc. From previous calculations,[44,45] for the free PbPc molecule, the overall "height" of the molecule (from the Pb atom to the hydrogen atoms of the benzene rings) is ~2.3 Å. These values are in good agreement with our DFT calculations for the free molecule where the molecular height was found to be 2.35 Å and the angle between the central hydrogen atoms and the central metal atoms was 107.6°. On adsorption on Ag(111), however, and as was also observed for SnPc, the DFT results show that there are significant distortions in the puckering of the Pc molecule as compared to the free molecule. As shown in Fig. 8, the PbPc molecule flattens substantially and the molecular plane becomes almost completely parallel to the Ag(111) surface. The Pb-Ag(111) distance determined from our DFT calculations is 2.76 Å.

Figure 9 is the (111) NIXSW profile for 1 ML of PbPc on Ag(111) (prepared, as for the other phthalocyanine molecules, via deposition onto a substrate held at 300 °C). The coherent position, D, extracted from a fit to the data is $0.2d_{\mathrm{Ag}(111)}$ or, given that NIXSW cannot distinguish between coherent positions which are separated by integer values of the plane spacing, $1.2d_{\mathrm{Ag}(111)}$ ($f_{co}=0.71 \pm 0.07$). A value of $0.2d_{\mathrm{Ag}(111)}$, i.e., 0.47 ± 0.05 Å is of course not consistent with a "Pb down" adsorption geometry of the molecule, assuming the Pb remains bound to the Pc macrocycle, as the Pb-Ag bond length is unphysically small. An alternative possibility (assuming a single adsorption geometry) is that the molecule adsorbs in a "Pb down" orientation with $D = 1.2d_{\mathrm{Ag}(111)} = 2.83 \pm 0.05$ Å. This would appear to be in good agreement with the DFT result (2.76 Å) but there are two key problems with this interpretation of the NIXSW data which we shall now discuss.

Figure 10 shows Pb $4f$ core-level spectra for a thick (bulklike) film of PbPc and a monolayer prepared by depositing the pthalocyanine molecules onto the Ag(111) substrate held at 300 °C. There is a clear shift of the Pb $4f$ core level by 2 eV to lower binding energy for the PbPc monolayer as compared to the spectrum for the thick PbPc film. A very similar shift of the Pb $4f$ core-level peaks to lower binding energy has been observed for thick vs thin films of PbPc

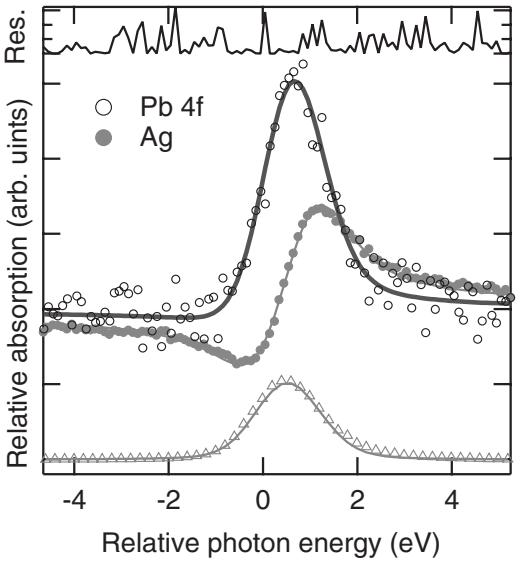

FIG. 9. Upper plots: (111) NIXSW profile for 1 ML of PbPc on Ag(111) (open circles). The dark gray line is a best fit to dynamical theory and yields a coherent position of $0.2d_{\mathrm{Ag(111)}}$ or $1.2d_{\mathrm{Ag(111)}}$ and a coherent fraction, f_{co}, of 0.71 ± 0.07. The NIXSW profile for the Ag(111) substrate is shown as the filled light gray circles. Lower plot: reflectivity curve.

deposited on both Pt(111)[46] and InSb(100).[47] In both cases, and as is also the case for the study described here, the 2 eV shift is indicative of a reduction in the lead from a Pb^{2+} oxidation state (for Pb in the free PbPc molecule) to a Pb^0 state. Papageorgiou *et al.*[46] interpreted this change in oxidation state to a strong interaction of the Pb atom with the Pt(111) surface (possibly involving the detachment of the Pb atom from the macrocycle) and the formation of a Pb-Pt alloy. They noted that this interpretation was supported by the observation that a Pb^0 core-level peak was still observed even after repeated cycles of Ar^+ sputtering of the Ag(111) surface and annealing under 0_2. Giovanelli *et al.*[47] had also studied PbPc but on a less reactive surface, InSb(100)-(4 $\times$2). They observed a similar reduction in the Pb atom upon annealing to 325 °C and also attributed it to a bonding with the substrate.

The second problem with an interpretation of the Pb 4*f* NIXSW data in terms of a single adsorption site with a Pb-

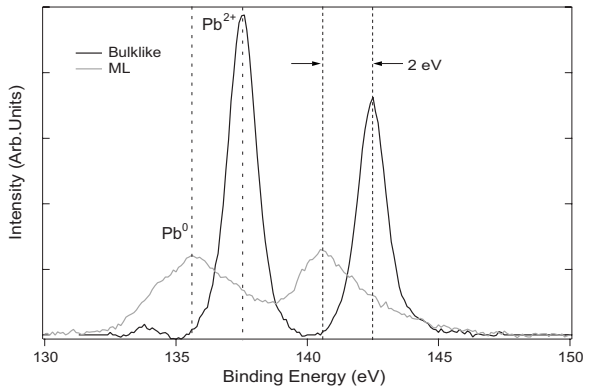

FIG. 10. Pb 4*f* XPS spectra of bulklike and monolayer films of PbPc on Ag(111).

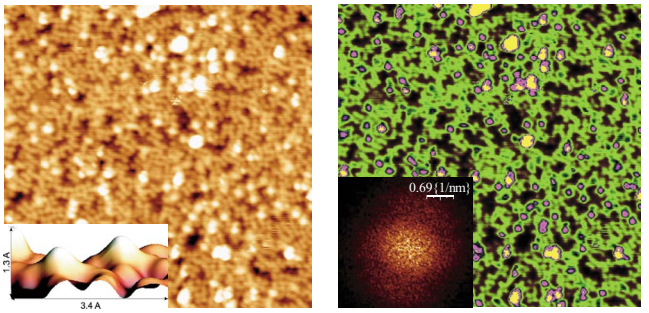

FIG. 11. (Color online) Left: a 35×35 nm^2 image of PbPc monolayer on Ag(111). Inset: a 3D topographic image of individual PbPc molecules. Right: The contrast has been enhanced to aid visualization of the up:down orientation. The majority of the image consists of the carbon macrocycle, shaded green. Inset: a Fourier transform of the image. Note the lack of any features in the transform. (Tunneling parameters: −1.5 V 0.2 nA)

Ag(111) bond distance of 2.83 Å relates to the C 1*s* NIXSW data for this system. The average position of the carbon atoms above the Ag(111) surface, as determined from C 1*s* NIXSW spectra, is 2.93 ± 0.05 Å with a coherent fraction of 0.49 ± 0.02. This is a great deal smaller than the value of 3.9 Å determined from DFT and, indeed, much smaller that the value of 3.61 ± 0.16 Å determined experimentally for the SnPc molecule on Ag(111) (using the "deposition onto a hot substrate" method of sample preparation). We propose that the anomalously low value of the average macrocycle-Ag(111) distance determined from the C 1*s* NIXSW data has a similar origin to the changes in the Pb 4*f* spectra discussed above and arises largely from the detachment of the Pb atom from the PbPc molecules. In addition, we find, perhaps somewhat surprisingly, that the coherent fraction associated with the carbon atoms of the PbPc molecules, 0.49 ± 0.02, is rather larger than the value of f_{co} measured for SnPc, 0.36 ± 0.09. The higher value of f_{co} observed for PbPc may possibly arise from a relaxation of the macrocycle following detachment of the Pb atom.

On the basis of the XPS data shown in Fig. 10, therefore, the best explanation for the M-Ag(111) *D* value we have measured for PbPc is that, in some cases, the Pb atom has detached from the Pc macrocycle due to a strong interaction with the Ag(111) surface. Dalmas *et al.*[48,49] had shown that Pb can form a two-dimensional Ag_2Pb surface alloy on Ag(111), despite the lower surface energy and larger atomic radius of Pb as compared to Ag. A simple interpretation of the measured ⟨111⟩ coherent position (~0.5 Å) as the "vertical" Pb-Ag separation within the surface alloy is, however, flawed because it is likely that there is a distribution of PbPc molecules in the "Pb down," "Pb up," and "Pb detached" states. Indeed, STM images of a PbPc/Ag(111) monolayer prepared via phthalocyanine deposition onto an Ag(111) surface held at 300 °C (Fig. 11), in addition to showing the presence of a poorly ordered Pc monolayer following adsorption of PbPc onto the Ag(111) surface (again, held at a temperature of 300 °C during deposition), show a distribution of bright features which may arise from a relatively small number of "Pb up"-oriented PbPc molecules. If we threshold the STM data as shown in Fig. 11(b), assuming

TABLE III. Calculated binding energies (in eV) for Sn-, Pb-, and Co phthalocyanine adsorption on Ag(111).

Configuration	SnPc	PbPc	CoPc
Hcp	1.26	0.71	
Fcc	1.06	0.59	
On-top			1.40
Bridge			1.28

that the brighter features in Fig. 11(a) arise from tunnelling into the Pb center of molecules adsorbed in the "Pb-up" geometry, then we can make a rough estimate of the total number of molecules adsorbed in the "Pb down" geometry, ~80%. This is broadly in line with the XPS data for the PbPc monolayer shown in Fig. 10 where it is clear that the majority of the Pb atoms are in a Pb^0 rather than Pb^2 oxidation state. A direct quantitative comparison of the STM and XPS data is problematic as the samples were prepared in different UHV systems and the error bar in the temperature measurements is ±30 °C in each case.

With our current data set it is thus not possible to ascertain definitively the relative numbers of "Pb up," "Pb down," and "Pb detached" molecules which comprise a PbPc monolayer on Ag(111). Suffice it to say that, contrary to the CoPc and SnPc cases, it appears clear that PbPc reacts with the Ag(111) surface at modest temperatures (~300 °C), with the Pb atom being reduced from its Pb^{2+} state in the free PbPc molecule to a Pb^0 state at the Ag(111) surface. The most plausible interpretation of our NIXSW, XPS, and STM data is that this reaction produces a surface Pb-Ag alloy, severely compromising the ability to form a well-ordered PbPc monolayer on the Ag(111) surface. It would, of course, be interesting to repeat the measurements for samples formed by deposition of PbPc onto an Ag(111) surface held at room or lower temperature.

V. COMPARISONS OF PHTHALOCYANINE ADSORPTION

A comparison of the binding energy of Pc molecules at various sites on the Ag(111) surface is given in Table III. Table II compares the values predicted by our DFT calculations for the separation of the metal atom and the carbon rings from the Ag(111) surface for CoPc, PbPc, and SnPc with those measured using NIXSW. There is excellent agreement between the DFT calculated and NIXSW-derived value of the Co-Ag(111) distance and a good match between the Sn-Ag(111) DFT calculation and NIXSW measurement (although the DFT value is outside of experimental error). Similarly, the average separation of the SnPc carbons from the Ag(111) surface as determined by DFT, 3.7 Å is in good agreement with that measured by NIXSW, 3.61±0.16 Å (albeit with a large experimental error bar). Metal-metal bond lengths are, however, generally overestimated with DFT. In addition, it is important to realize that the DFT calculations do not treat van der Waals interactions correctly, which means that any additional nonbonded interaction between the surface and the macrocycle is underestimated.

Our calculations show that all three MPc molecules investigated in this study bind to the Ag(111) substrate through the metal atom M (M=Co,Sn,Pb). To better understand the interaction between the phthalocyanine molecules and the silver surface, we plot the frontier orbitals of each of the molecules and compare their energies to our calculated Ag(111) Fermi level[50,51] (Fig. 12). As can be seen, the Fermi level crosses the HOMO-LUMO gap for SnPc and PbPc but is between the LUMO and LUMO+1 levels for CoPc. We have tracked the modification of the molecular orbitals of the free molecules upon interaction with the substrate by means of PDOS plots (Fig. 13).

To describe charge transfer at the MPc/Ag(111) interface we have analyzed the charge-density distribution using Mulliken population analysis. The definition of Mulliken charges has its limitations but, when used correctly, can still give useful information about partial atomic charges. Table IV shows the charges of the central metal atom and Pc ligand for free and adsorbed MPc and the charge on the silver cluster after adsorption. All molecules in this study donate electrons to the Ag surface, resulting in accumulation of electron density below the absorbed molecules, in agreement with the speculated charge transfer for SnPc bonded to Ag(111).[14] From Table IV we can draw the conclusion that the donated electronic charge is from the Pc macrocycle to silver, amounting to 1.39, 1.01, and 0.45 electrons for CoPc, SnPc, and PbPc, respectively. This could be achieved through both depopulation of the HOMO or donating bonds (dative bonding) of occupied Pc-dominated MOs and the surface mediated by the central metal atom M=Co, Sn, Pb (e.g., HOMO-1). Inspection of Fig. 13 shows that the charge transfer is mainly through the latter mechanism since no depopulation of the HOMO is seen in either the Pc PDOS of SnPc or PbPc. On the contrary, one can see a partial population of the Pc-dominated LUMO in SnPc when surface bound (as referred to in relation to unpublished UPS data in Ref. 14). In CoPc there is in addition considerable back donation from Ag to Co (0.44 electrons) by population of its LUMO, which is lower in energy than the Ag Fermi level (see Fig. 12), and is connected to the quenching of the CoPc magnetic moment when the molecule is surface bound (see Fig. 5). The occupation of the CoPc LUMO, which is a spin orbital, results in a formal reduction in the oxidation state from Co(II) to Co(I) upon binding to Ag(111). Such backdonation to the central metal atom is negligible in SnPc and PbPc (amounting to 0.11 electrons for both molecules).

Both SnPc and PbPc possess a lone pair oriented along the fourfold axis. This feature, and the shuttlecock shape of the molecules, gives rise to a directional anisotropy and dictates their adsorption geometry on different substrates.[52] The lone pair has mixed s and p character and corresponds to the HOMO-1 orbital (see Fig. 12). On adsorption we find that both SnPc and PbPc bind to the two hollow binding sites (i.e., fcc and hcp). The metal ion PDOS changes considerably (see Fig. 13), which indicates strong mixing of the Sn and Pb orbitals with sp and d bands of Ag(111).

The Sn atom coordinates with the silver states largely via its HOMO-1 orbital. In addition, coordination by the 4d orbital for Sn and, similarly, the 5d and 4f orbitals for Pb is also present and provides valuable physical and chemical

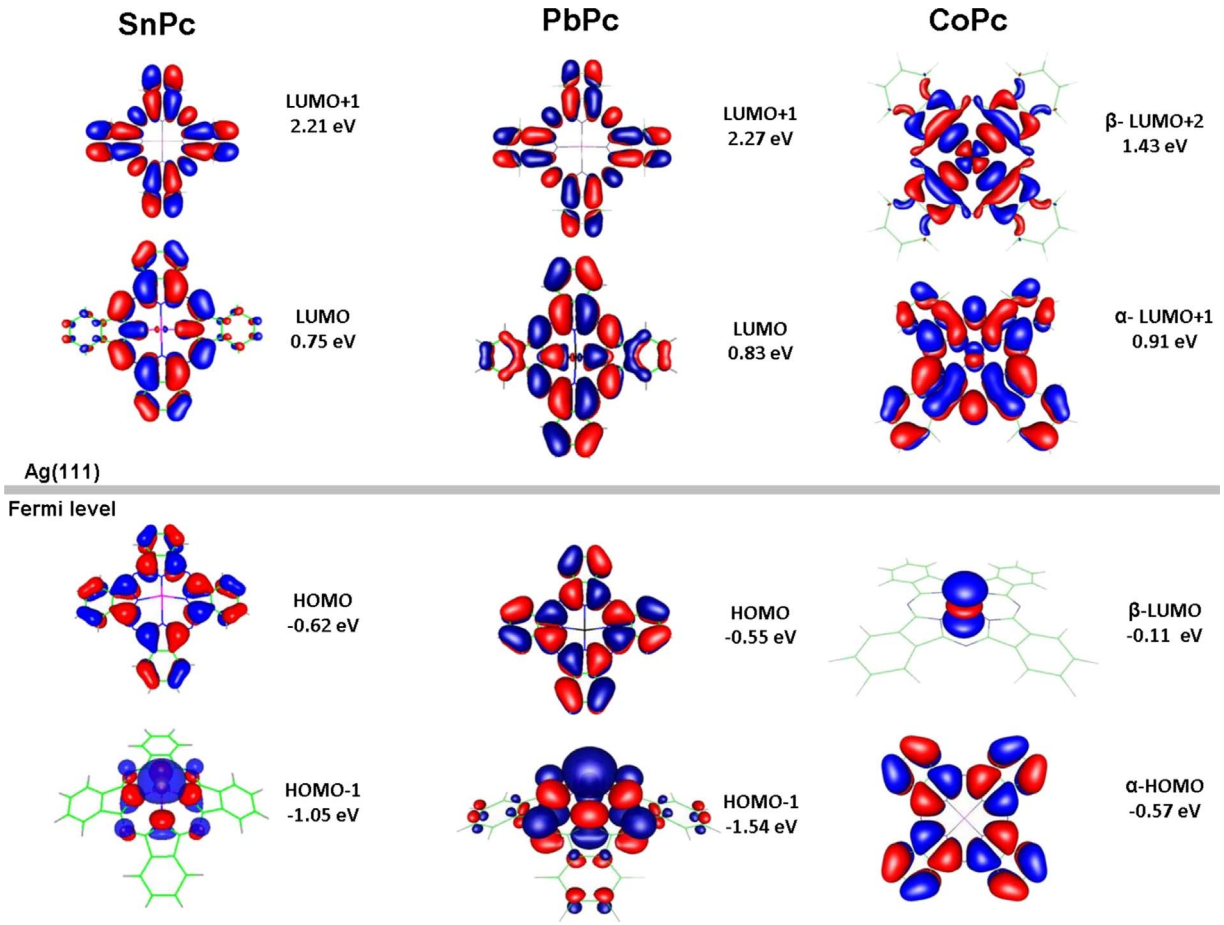

FIG. 12. (Color online) Representation of the frontier orbitals of free SnPc, PbPc, and CoPc for an isovalue of $\pm 0.015(e-/\text{Å}^3)^{1/2}$. The energy value in each case is relative to the Fermi level of the Ag(111) cluster. For clarity we show only one of the e orbitals of the LUMO+1 state of the CoPc molecule.

information about the nature of the molecule-surface interaction.[44] When bound to either the hcp or fcc hollow site, the Sn and Pb orbitals can overlap with those of the surface most effectively. Our calculations reveal that the extra stabilization on the hcp-hollow site over the fcc-hollow site comes from an overlap of the central metal orbitals with the d_{z_2} orbital of a second layer Ag atom. The difference in the puckering of the free and adsorbed SnPc and PbPc molecules show also that the phthalocyanine π system is strongly affected by binding to the Ag(111) surface, as has been seen for other molecules.[53–55] The PDOS of the SnPc ligand shows a downshift in energy, which can be assigned to a charge redistribution, and arises from a significant interaction between the Sn atom and the Ag surface leading to a loss of electrons for Sn (reduction in Sn PDOS peaks) close to the Fermi level, and subsequent transfer of electrons from the macrocycle to Sn, resulting in an effective charge transfer from Pc to Ag(111). This down shift in energy for the Pc ligand is also observed for CoPc, and to a lesser degree for PbPc, when bonded to Ag(111).

VI. CONCLUSIONS

We have carried out a comparative study of the adsorption of three phthalocyanine molecules, CoPc, SnPc, and PbPb, on Ag(111) using a range of experimental techniques coupled with DFT calculations. There are very strong differences in the adsorption behavior of each of the Pc molecules on Ag(111). Although in each case adsorption is driven by the interaction of the central metal atom with the Ag(111) surface, we find that only SnPc forms a long range ordered

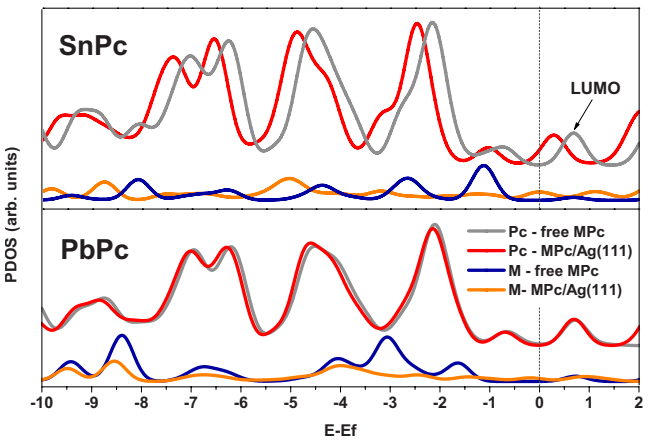

FIG. 13. (Color online) PDOS of the ligand and the central metal of SnPc and PbPc for a free molecule and adsorbed on Ag(111).

TABLE IV. Charges of the central metal atom and Pc ligand of free CoPc, SnPc, and PbPc and charge on silver cluster after adsorption for the most stable adsorption configuration.

	Co	Pc	Sn	Pc	Pb	Pc
Free	+0.64	−0.64	+0.64	−0.64	+0.73	−0.73
Surface bound	+0.20	+0.75	+0.53	+0.37	+0.62	−0.28
Ag cluster		−0.95 (CoPc)		−0.90 (SnPc)		−0.34 (PbPc)

monolayer (using the monolayer preparation technique we have used). CoPc forms a locally ordered monolayer whereas for the preparation conditions used in our experiments (deposition onto a substrate held at 300 °C), we did not observe ordering of PbPc molecules in our STM data. We attribute this to a strong interaction of the central Pb atom with the Ag(111) surface, visible as a shift from an apparent oxidation state of +2 to 0 in XPS spectra, and leading to the formation of a Pb-Ag surface alloy. We find good agreement between the *M*-Ag(111) distances determined by NIXSW measurements and those predicted by DFT for CoPc and SnPc. Similarly, simulated STM images of CoPc/Ag(111) capture the key features of the experimental STM data and highlight the role that the Co 3*d* orbitals play in image contrast.

For all three MPc molecules, our DFT results indicate that electronic charge is donated from the Pc macrocycle to the Ag(111) surface mediated by the central metal atom. For CoPc there is in addition a significant backdonation from the substrate to the Co atom, through population of the CoPc LUMO which is lower in energy than the Ag Fermi level. The highest degree of charge transfer is observed for CoPc. Significant differences in molecular geometry—in particular, the "flattening" of the phthalocyanine framework for SnPc and PbPc—are observed for the adsorbed, as compared to the free molecule. Similarly, the electronic structure of the adsorbed phthalocyanine can differ considerably form that of the free molecule—the magnetic moment of CoPc, for example, is quenched upon adsorption on Ag(111). Finally, although the interaction between each MPc molecule and the Ag(111) surface is dominated by *M*-Ag bonding, an important unaddressed question in our study relates to the contribution of dispersion forces to the total molecule-substrate adsorption energy. We are keen to extend our work to incorporate dispersion interactions within the DFT framework, as has been demonstrated by a number of groups recently.[56–59]

ACKNOWLEDGMENTS

We acknowledge funding from the European Union's Framework 6 Programme: Marie Curie Early Stage Training, Contract No. MRTN-CT-2004-506854 (NANOCAGE), the SFI/HEA Irish Centre for High End Computing (ICHEC) for the provision of computational facilities, and SFI/HEA for the provision of local computing clusters. K.S. thanks the University of Nottingham for support from the Anne McLaren foundation. A.A.C. acknowledges funding from the Higher Education Authority's Programme for Research in Third-level Institutions (PRTLI Cycle II) and from Science Foundation Ireland (Grant No. 06/RFP/PHY082).

[1] S. R. Forrest, Chem. Rev. (Washington, D.C.) **97**, 1793 (1997).
[2] R. Strohmaier, C. Ludwig, J. Petersen, B. G ompf, and W. Eisenmenger, J. Vac. Sci. Technol. B **14**, 1079 (1996).
[3] T. Angot, E. Salomon, N. Papageorgiou, and J.-M. Layet, Surf. Sci. **572**, 59 (2004).
[4] M. Lackinger and M. Hietschold, Surf. Sci. **520**, L619 (2002).
[5] C. Stadler, S. Hansen, F. Pollinger, C. Kumpf, E. Umbach, T.-L. Lee, and J. Zegenhagen, Phys. Rev. B **74**, 035404 (2006).
[6] R. A. J. Woolley, C. P. Martin, G. Miller, V. R. Dhanak, and P. J. Moriarty, Surf. Sci. **601**, 1231 (2007).
[7] J. Ahlund, J. Schnadt, K. Nilson, E. Gothelid, J. Schiessling, F. Besenbacher, N. Martensson, and C. Puglia, Surf. Sci. **601**, 3661 (2007).
[8] C. C. Leznoff and A. B. P. Lever, *Phthalocyanines: Properties and Applications* (VCH, New York, 1989–1996), Vols. 1-4.
[9] J. K. Gimzewski, E. Stoll, and R. R. Schlittler, Surf. Sci. **181**, 267 (1987).
[10] P. H. Lippel, R. J. Wilson, M. D. Miller, C. Woll, and S. Chiang, Phys. Rev. Lett. **62**, 171 (1989).
[11] A. Zhao, Q. Li, L. Chen, H. Xiang, W. Wang, S. Pan, B. Wang, Z. Xiao, J. Yang, J. G. Hou, and Q. Zhu, Science **309**, 1542 (2005).
[12] Y. Wang, J. Kröger, R. Berndt, and W. A. Hofer, J. Am. Chem. Soc. **131**, 3639 (2009).
[13] A. Gerlach, F. Schreiber, S. Sellner, H. Dosch, I. A. Vartanyants, B. C. C. Cowie, T.-L. Lee, and J. Zegenhagen, Phys. Rev. B **71**, 205425 (2005).
[14] C. Stadler, S. Hansen, I. Kroger, C. Kumpf, and E. Umbach, Nat. Phys. **5**, 153 (2009).
[15] B. N. Figgis, E. S. Kucharski, and P. A. Reynolds, J. Am. Chem. Soc. **111**, 1683 (1989).
[16] V. V. Maslyuk, V. Y. Aristov, O. V. Molodtsova, D. V. Vyalikh, V. M. Zhilin, Y. A. Ossipyan, T. Bredow, I. Mertig, and M. Knupfer, Appl. Phys. A: Mater. Sci. Process. **94**, 485 (2009).
[17] K. Leung, S. B. Rempe, P. A. Schultz, E. M. Sproviero, V. S. Batista, M. E. Chandross, and C. J. Medforth, J. Am. Chem. Soc. **128**, 3659 (2006).
[18] C. Iacovita, M. V. Rastei, B. W. Heinrich, T. Brumme, J. Kortus, L. Limot, and J. P. Bucher, Phys. Rev. Lett. **101**, 116602 (2008).
[19] R. Ahlrichs, M. Bär, M. Häser, H. Horn, and C. Kölmel, Chem. Phys. Lett. **162**, 165 (1989).
[20] J. P. Perdew, K. Burke, and M. Ernzerhof, Phys. Rev. Lett. **77**,

3865 (1996).
[21] K. Eichkorn, O. Treutler, H. Öhm, M. Häser, and R. Ahlrichs, Chem. Phys. Lett. **242**, 652 (1995).
[22] K. Eichkorn, F. Weigend, O. Treutler, and R. Ahlrichs, Theor. Chem. Acc. **97**, 119 (1997).
[23] D. Andrae, U. Haeussermann, M. Dolg, H. Stoll, and H. Preuss, Theor. Chim. Acta **77**, 123 (1990).
[24] B. Metz, H. Stoll, and M. Dolg, J. Chem. Phys. **113**, 2563 (2000).
[25] D. P. Woodruff, Prog. Surf. Sci. **57**, 1 (1998).
[26] R. G. Jones, A. S. Y. Chan, M. G. Roper, M. P. Skegg, I. G. Shuttleworth, C. J. Fisher, G. J. Jackson, J. J. Lee, D. P. Woodruff, N. K. Singh, and B. C. C. Cowie, J. Phys.: Condens. Matter **14**, 4059 (2002).
[27] J. Zegenhagen, Surf. Sci. Rep. **18** (7-8), 202 (1993).
[28] C. J. Fisher, R. Ithin, R. G. Jones, G. J. Jackson, D. P. Woodruff, and B. C. C. Cowie, J. Phys.: Condens. Matter **10**, L623 (1998).
[29] D. P. Woodruff, Rep. Prog. Phys. **68**, 743 (2005).
[30] I. A. Vartanyants and J. Zegenhagen, Solid State Commun. **113**, 299 (1999).
[31] J. J. Lee, C. J. Fisher, D. P. Woodruff, M. G. Roper, R. G. Jones, and B. C. C. Cowie, Surf. Sci. **494**, 166 (2001).
[32] F. Schreiber, K. A. Ritley, I. A. Vartanyants, H. Dosch, J. Zegenhagen, and B. C. C. Cowie, Surf. Sci. **486**, L519 (2001).
[33] R. A. J. Woolley, K. H. G. Schulte, L. Wang, P. J. Moriarty, B. C. C. Cowie, H. Shinohara, M. Kanai, and T. J. S. Dennis, Nano Lett. **4**, 361 (2004).
[34] K. Schulte, R. A. J. Woolley, L. Wang, P. J. Moriarty, P. R. Birkett, H. W. Kroto, and B. C. C. Cowie, Nucl. Instrum. Methods Phys. Res. A **547**, 208 (2005).
[35] S.-H. Chang, S. Kuck, J. Brede, L. Lichtenstein, G. Hoffmann, and R. Wiesendanger, Phys. Rev. B **78**, 233409 (2008).
[36] S. Berner, M. de Wild, L. Ramoino, S. Ivan, A. Baratoff, H. J. Güntherodt, H. Suzuki, D. Schlettwein, and T. A. Jung, Phys. Rev. B **68**, 115410 (2003).
[37] K. Walzer and M. Hietschold, Surf. Sci. **471**, 1 (2001).
[38] M. Böhringer, R. Berndt, and W.-D. Schneider, Phys. Rev. B **55**, 1384 (1997).
[39] X. Lu and K. W. Hipps, J. Phys. Chem. B **101**, 5391 (1997).
[40] X. Lu, K. W. Hipps, X. D. Wang, and U. Mazur, J. Am. Chem. Soc. **118**, 7197 (1996).
[41] T. Lukasczyk, K. Flechtner, L. R. Merte, N. Jux, F. Maier, J. M. Gottfried, and H.-P. Steinruck, J. Phys. Chem. C **111**, 3090 (2007).
[42] Z. P. Hu, B. Li, A. D. Zhao, J. L. Yang, and J. G. Hou, J. Phys. Chem. C **112**, 13650 (2008).
[43] F. Song *et al.*, J. Phys.: Condens. Matter **19**, 136002 (2007).
[44] N. Papageorgiou, Y. Ferro, E. Salomon, A. Allouche, J. M. Layet, L. Giovanneli, and G. Le Lay, Phys. Rev. B **68**, 235105 (2003).
[45] P. N. Day, Z. Q. Wang, and R. Pachter, J. Mol. Struct.: THEOCHEM **455**, 33 (1998).
[46] N. Papageorgiou, J. C. Mossoyan, M. Mossoyan-Deneux, G. Terzian, E. Janin, M. Gothelid, L. Giovanelli, J. M. Layet, and G. Le Lay, Appl. Surf. Sci. **162-163**, 178 (2000).
[47] L. Giovanelli, N. Papageorgiou, G. Terzian, J. M. Layet, J. C. Mossoyan, M. Mossoyan-Deneux, M. Gothelid, and G. Le Lay, J. Electron Spectrosc. Relat. Phenom. **114-116**, 375 (2001).
[48] J. Dalmas, H. Oughaddou, C. Leandri, J. M. Gay, G. Le lay, G. Treglia, B. Aufray, O. Bunk, and R. L. Johnson, J. Phys. Chem. Solids **67**, 601 (2006).
[49] J. Dalmas, H. Oughaddou, C. Leandri, J. M. Gay, G. Le Gay, G. Treglia, B. Aufray, O. Bunk, and R. L. Johnson, Phys. Rev. B **72**, 155424 (2005).
[50] G. Mattioli, F. Filippone, P. Giannozzi, R. Caminiti, and A. A. Bonapasta, Phys. Rev. Lett. **101**, 126805 (2008).
[51] D. Lamoen, P. Ballone, and M. Parrinello, Phys. Rev. B **54**, 5097 (1996).
[52] N. Papageorgiou, E. Salomon, T. Angot, J.-M. Layet, L. Giovanelli, and G. L. Lay, Prog. Surf. Sci. **77**, 139 (2004).
[53] Y. Zou, L. Kilian, A. Scholl, T. Schmidt, R. Fink, and E. Umbach, Surf. Sci. **600**, 1240 (2006).
[54] A. Ferretti, C. Baldacchini, A. Calzolari, R. Di Felice, A. Ruini, E. Molinari, and M. G. Betti, Phys. Rev. Lett. **99**, 046802 (2007).
[55] L. Romaner *et al.*, Phys. Rev. Lett. **99**, 256801 (2007).
[56] M. Dion, H. Rydberg, E. Schroder, D. C. Langreth, and B. I. Lundqvist, Phys. Rev. Lett. **92**, 246401 (2004).
[57] S. D. Chakarova-Käck, E. Schroder, B. I. Lundqvist, and D. C. Langreth, Phys. Rev. Lett. **96**, 146107 (2006).
[58] S. Grimme, J. Comput. Chem. **27**, 1787 (2006).
[59] N. Atodiresei, V. Caciuc, P. Lazic, and S. Blugel, Phys. Rev. Lett. **102**, 136809 (2009).